Settling of the COVID-19 Virus in Air and Some Observations on Face Masks

Michael M. Ellis* and Stephen D. Antolovich**

Abstract

The goals of this study have been: (a) to examine how the SARS-CoV-2 virus, commonly referred to as COVID-19, can enter into the local environment from breathing, talking, coughing and sneezing, (b) to examine the likely effectiveness of masking, and (c) to provide neutral information to help in making good public health decisions. Calculations were done using well-established physics principles and reliable, modern data sources. Stokes Law for settling was used and shows that the time for the average sized virus (~100-120 nm) to fall one metre in relatively dry air (30% relative humidity at one atmosphere (atm) pressure and 25 ^{o}C (77 ^{o}F)) is about 26 days with a range of 149 days (50 nm virus) to 2.33 days (200 nm virus). The effect of virus encapsulation by saliva was also considered. The measured distributions of saliva droplets in a sneeze and saliva evaporation rates were used to calculate the effect of evaporation on COVID-19 settling times. Even for the saliva-covered COVID-19 virions, which are much larger than the "dry" virions, the settling time is sufficiently mediated by evaporation to still allow for complete evaporation before falling one metre. Increases in relative humidity had but a small effect on increasing the settling times. However, increasing the temperature to 37^{o}C (98.6^{o}F) markedly reduced the settling times of droplets for full evaporation. Thus, viruses under various conditions, are released into the local environment. The efficacy of currently available masks (from home-made masks of various types and materials to N-95) is considered in terms of their physical characteristics. We found no instance in which currently available masks were either designed for or capable of reliably filtering viruses. The possibility of masking as a strategy for dealing with the spread of COVID-19 is considered and suggestions are made for improved approaches.

Subject Areas: Fluid Mechanics, Filtration, Bio-Engineering, Bio-Physics, Bio-Mechanics, COVID-19

Key Words: Stokes Law, Size Distribution, Droplet Evaporation, Effect of Temperature, N-95 Face Mask, Face Masks, SARS-CoV-2, COVID-19, Infectious Disease, Airborne Infection, Sneezing, Coughing, Talking, Breathing

*Advanced Materials Engineering, USA
**Georgia Institute of Technology, Atlanta, Georgia USA & Washington State University, Pullman, Washington USA

Corresponding Author: M.M. Ellis, mellis@advancedmaterialsengineering.com

Outline of Paper

Symbols Used

v = settling velocity of terminal velocity of COVID-19 particle [m/sec].
ρ_v, ρ_a = density of the falling particle and media containing particle respectively [kg/m^3].
g = acceleration due to gravity [m/sec^2].
R = radius of settling particle [m]. Sometimes [nm] or [μm] depending on context.
μ = viscosity of the media in which the particle is falling (in this case, air) [kg/m/sec].
C = saliva evaporation rate [m^2/sec]
D_o, D = initial and diameter at any time of settling particle. Same units as R [m] etc.
A = surface area of virus-containing droplet [m^2]
$\Delta\rho$ = difference in density between virus or virus/droplet and air [kg/m^3].
RH = relative humidity [%]
HEPA = high efficiency particulate air filter
ULPA = ultra-low particulate air filter ULPA
F_Σ = the sum of buoyant forces [N]
F_p = force associated with momentum advection [N]
G1 = flux of particles flowing into the filter
G2 = flux of particles emitted by the filter and not trapped
G3 = portion of the particles trapped by the filter
E = filter efficiency [fraction] (or, sometimes, %)
P_n = penetration of filter medium.[fraction]
P^* = reduction in particle concentration after passing through the filter [fraction]
Q^* = filter efficiency [fraction]

I. Introduction

Since the outbreak of the severe acute respiratory syndrome corona virus -2 (SARS-CoV-2), more commonly referred to as COVID-19, social distancing and the wearing of face masks have become ubiquitous in an attempt to impede the spread of this beta-corona virus by direct and indirect contacts or airborne transmission. In this paper we examine the utility of these measures in actually safeguarding people from the spread of this or any other virus and suggest potential improvements. We make no comments whatsoever on the mechanisms of actual infection or any epidemiological considerations. We begin by reviewing what is currently known about COVID-19 and other viruses, in particular, considering the size of the virus and properties of a range of masks. We next consider a general overview of the approaches currently being taken to stop the spread of the virus. In the following section we analyse the time for both "raw" and saliva encapsulated viruses to fall one metre. We also analyse the effect of evaporation on the settling time of saliva encapsulated COVID-19 virions. We end by drawing conclusions based on our analysis and make several suggestions for research aimed at reducing the physical spread of the virus.

II. Properties and Calculations of Settling Rates of COVID-19 Virions

A. Properties of Covid-19 and Other Viruses

Transmission electron microcopy on negative-stained samples of the 2019 SARS-CoV-2 revealed a diameter size distribution ranging from 60 to 140 nm with the glycoprotein peplomers ranging in sizes from 9 to 12 nm [1]. SARS-CoV-2 is generally spheroidal in shape with the virion displaying pleomorphic morphology as shown in the two transmission electron micrographs (TEM) below [1].

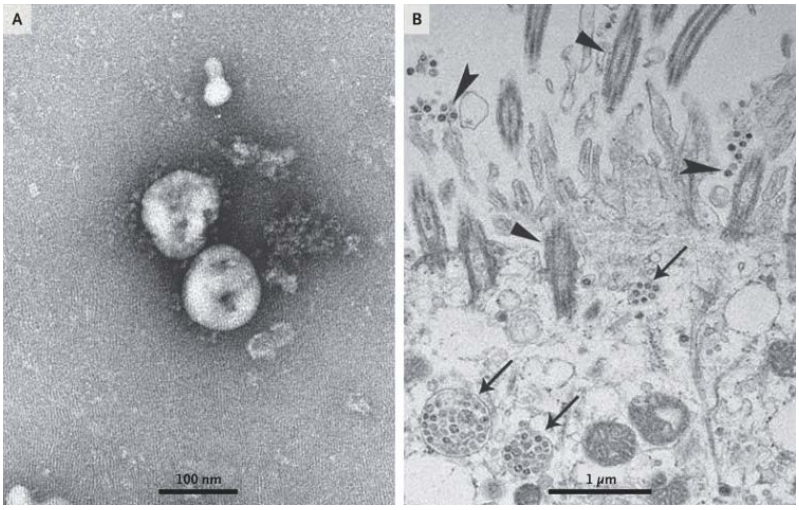

Fig. 1. Transmission electron micrograph of negative-stained samples of the 2019 SARS-CoV-2 revealed a diameter size distribution ranging from 60 to 140 nm with the glycoprotein peplomers ranging in sizes from 9 nm to 12 nm. Generally spherical with some pleomorphism [1]. See Appendix D for a photo of white blood cells and COVID-19 virions.

In order to gain a better understanding of the very small size of the SARS-CoV-2 virus, a comparison with electromagnetic radiation is appropriate. The human eye detects and perceives as visible light electromagnetic wavelengths between 380 nm and 760 nm (violet to red light) [2,3]. Ultraviolet radiation wavelengths range from the near ultraviolet (NUV) at 400-300 nm to the

middle ultraviolet (MUV) range at 300-200 nm to the far ultraviolet (FUV) scale at 200-100 nm, to the extreme ultraviolet (EUV) range at 100 nm to 10 nm [2,3]. Ten nm is where soft X-ray radiation starts and ends at hard X-rays with a wavelength of 10 pm, the beginning of gamma radiation [2,3]. Thus, the size of the SARS-CoV-2 virus lies between the far ultraviolet range and the extreme ultraviolet scale, making this virus much smaller than the visible light wavelength. This is illustrated in Fig. 2.

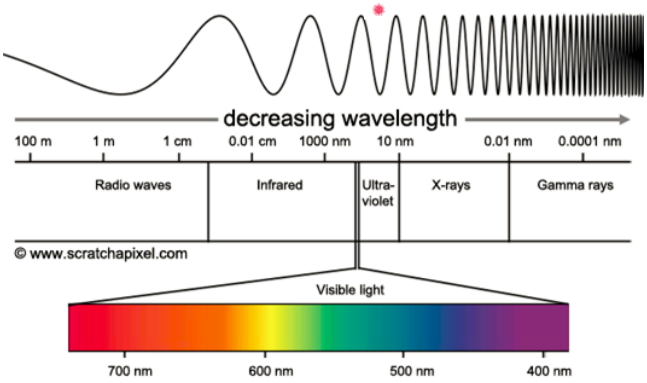

Fig. 2. Electro-magnetic spectrum. The COVID-19 virus is shown schematically in the ultraviolet range as a red dot on the top drawing.

B. Calculation of Settling Rates of COVID-19 Virions

Any rational approach to mitigation of the effects of Covid-19 infection requires, as a starting point, knowledge of the distribution of the COVID-19 virions. Coughing, sneezing, and talking are widely considered to be the primary mechanisms of spreading the virions. The question naturally arises as to how long the virions remain in the environment and what is their nature. The motion of "dry" and "wet" virions must be considered; three settling cases of interest have been considered:

- Falling of the "dry" virus in dry air
- Falling of saliva-covered "wet" virus ignoring evaporation.
- Falling of saliva-covered "wet" virus with simultaneous evaporation.

These cases are considered in the following sections[a].

1. Settling of Dry COVID-19 Virions

One can calculate the time that it takes to drop, for example, one metre using the well-established Stokes Law [4,5]. In this formulation, the gravitational force on a particle in a media (either liquid or gas) is balanced by buoyant forces on the particle plus the viscous forces acting at the particle/media interface. The balance of these forces is used to calculate the terminal velocity with the result:

$$v = \frac{2}{9}(\rho_v - \rho_a) g R^2 / \mu \qquad \ldots \text{(Eq. 1)}$$

[a] The calculations ignore the additional retarding effects of the peplomers located on the viral envelope.

Where:

v = terminal velocity
ρ_v, ρ_a = density of the falling particle and media containing particle respectively
g = acceleration due to gravity
R = radius of settling particle
μ = viscosity of the media in which the particle is falling (in this case, air)

In all cases numerical calculations were carried out in the SI system as shown in Table 1 where the units and magnitudes of the quantities in Eq.1 are also shown.

Equation 1 was evaluated using data obtained from the open literature [6], [7], [8] as given in Table 1. The density of the virus has been taken as the average of values presented in [6] and [8]. This choice has but a minor effect on the results, as opposed to using any of the specific values in these studies.

Table 1. Settling of Dry Virus in Dry Air at 298°K (77°F) and 1 Atm Pressure. Computed values are shown in red.

Calculated Steady State Falling Rate of Corona Virus in Dry Still Air at 298K and 1 Atmosphere Pressure									
Stokes Law: basis for calculation		Virus Density ρ_v (kg/m^3)	Dry Air Density ρ_a (kg/m^3)	Acceleration of Gravity g (m/sec^2)	Virus Radius R (m)	Dynamic Viscosity of Air μ (kg/sec/m)	Virus Diameter D (nm)	**Terminal Velocity v (m/sec)**	**Time to Fall One Metre (days)**
$v = 2/9(\rho_v - \rho_a)gR^2/\mu$									
		1.06E+03	1.184	9.8	2.50E-08	1.849E-05	50	**7.79E-08**	**148.49**
					5.00E-08		100	**3.12E-07**	**37.12**
					7.50E-08		150	**7.01E-07**	**16.50**
					1.00E-07		200	**1.25E-06**	**9.28**
					1.25E-07		250	**1.95E-06**	**5.94**
					1.50E-07		300	**2.81E-06**	**4.12**
					1.75E-07		350	**3.82E-06**	**3.03**
					6.00E-08		120	**4.49E-07**	**25.78**
					2.00E-07		400	**4.99E-06**	**2.32**

A graph of the results shown in Table 1 is given in Fig. 3. Figure 3 shows typical Stokes Law behaviour of decreasing settling time with increasing particle size. Given that the size of the virus ranges from 60 nm to 140 nm with an average of between 100/120 nm [1], we use 120-nm for purposes of discussion[b]. At this size, the time to fall 1 metre is about 26 days. Since the calculation was performed using assumptions favouring a faster settling rate, this number can be

[b] Using the upper limit of the average size will bias the results slightly towards a faster settling rate and a shorter time to fall one metre.

viewed as a minimum time the virus is in the air. Importantly, the lifetime of the airborne virus[c] has been shown to be from 0.64 to 2.64 hrs. with a mean of 1.09 hrs. [9] which means that: (a) "dry" virions will always be in the air, and (b) most of them will be dead. Presumably dead virions have no deleterious effects and furthermore may well have a positive effect when it is recalled that dead virions are the basis of many vaccines. The fact that virions are always in the air suggests that appropriate masking might be an effective strategy for combating the spread of the virus.

The effects of sneezing and coughing are considered in the following sections.

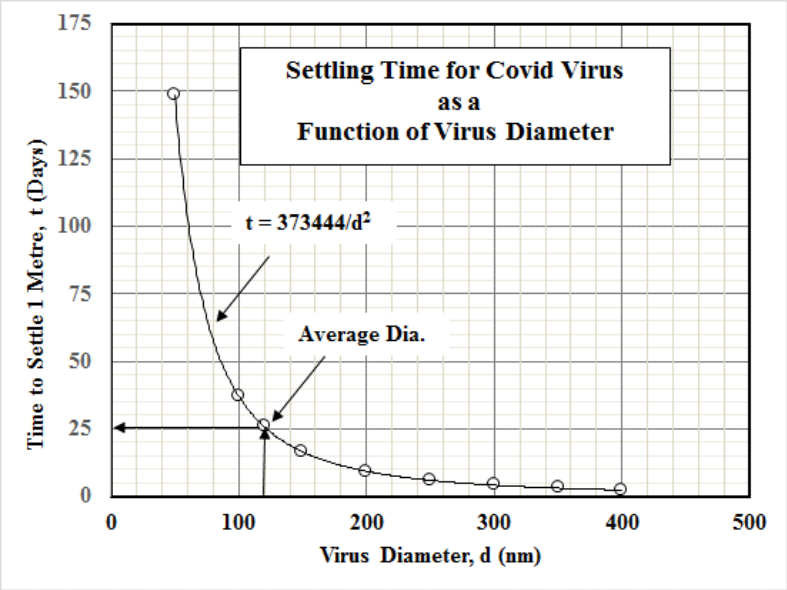

Fig. 3. Calculated time for a "dry" COVID-19 virus to settle 1 metre in dry air at 298K and 1 atm pressure according to Stokes Law. The range of observed COVID-19 size range is 60 nm-140 nm. The open and closed circles on Figs. 3,7,9 and 10 represent points at which calculations were made and are not experimental data.

2. Wet COVID-19 Virions; Coughing and Sneezing in Still air at 298K

Coughing and sneezing are mechanisms for emitting saliva-coated virions into the air. Two cases are considered: (a) a simplified calculation in which evaporation effects are ignored and (b) a more realistic calculation in which evaporation effects are considered. In case (b) the rate at which the droplets fall will decrease since the "particle" is constantly becoming smaller as it falls through the air.

a. Settling of Saliva-Encapsulated COVID-19 Virions – Evaporation Ignored

The size and distribution of sneeze particles has been measured recently [10] as shown in Fig. 4. An idealized distribution for the bimodal distributions is shown in Fig. 5.

[c] This letter also shows virions can remain viable for as short a time as 0.77 hrs. on Cu and for as long as 8.17 hrs. on plastic and in-between times on other surfaces.

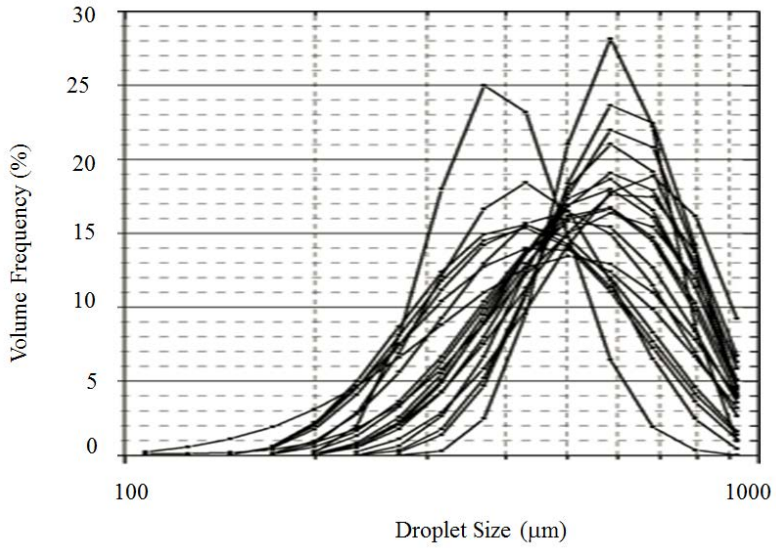

(a)

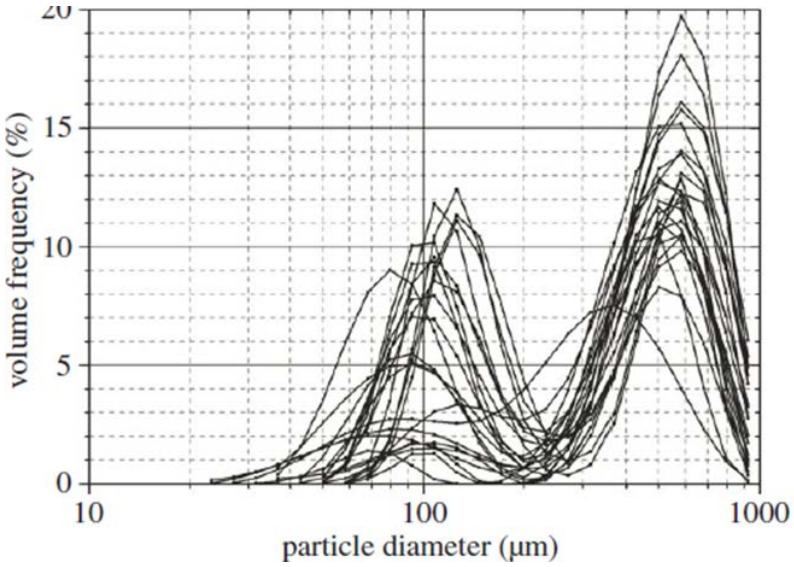

(b)

Fig. 4. Distribution of droplet sizes in sneezes from several subjects showing (a) unimodal and (b) bi-modal distributions [10]. Note that the distribution is given in terms of the volume frequency which will shift peaks to larger sizes.

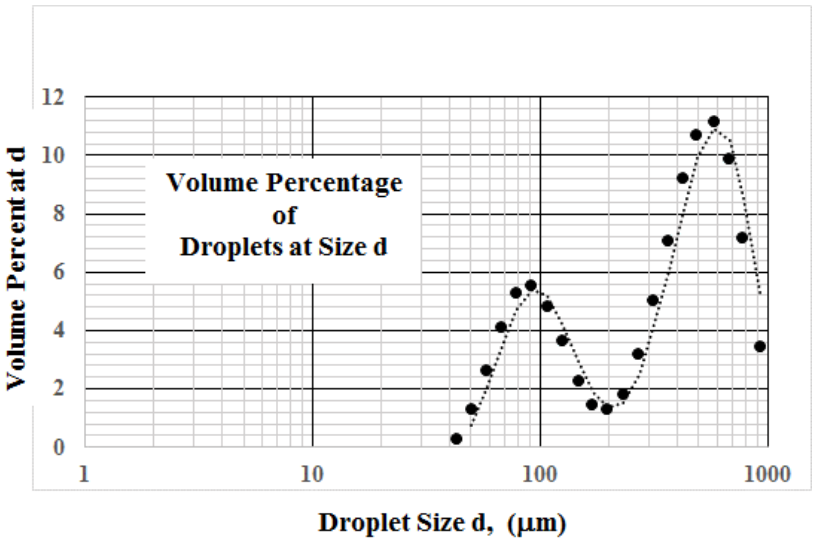

Fig. 5. Idealized bimodal distribution of droplets. Data taken from [10]. The dotted line was constructed using the running average as an aid in visualizing data trends.

Since the actual concentration of COVID-19 virions within droplets is not known to any degree of precision, it would be of value to recast the results of the droplet distributions in terms of number fraction. This is equivalent to counting every droplet equally in terms of the virion distribution. This method places equal weight on all droplet sizes whereas the volume fraction method places more weight on the larger particles which are most likely to fall to a surface much sooner than the smaller droplets. This can be done by using a representative volume, calculating the total volume of droplets at any size and then dividing by the volume of a single droplet at the size of interest. This procedure was carried out using the data used to construct Fig. 5. The results are shown in Table 2 and graphically in Fig. 6. Next, Stokes Law, Eq. 1, was used to produce a graph of the droplet size vs the time to fall 1 metre as shown in Fig. 7. Figure 7 shows that the saliva-encased virions settle in very short times. In particular, the settling time at the largest number of particles is around 9 seconds as opposed to 26 days for representative dry virions, Fig. 3. This number tends to indicate that "wet" virions: (a) fall rapidly and (b) could possibly be effectively blocked by an appropriately sealed mask. At the smallest virus size measured, the settling rate is approximately 21 seconds, far less than the 25 days for dry virions. This means that "wet" virions would be in the air for a short time before falling on a surface. Clearly surfaces would act as traps for the COVID-19 virus if, in fact, some other process didn't somehow promote drying of the virions. Such a process could be evaporation, considered in the following section.

Table 2. Calculation of the Number Percent of Droplets in Representative Sneeze Using Data from Ref [10].

Droplet Size, d (m)	Droplet Volume, vp (m^3)	Volume Per Cent (%)	Number Per Cent of Droplets at size d
4.31E-05	4.178E-14	0.248	4.77
5.02E-05	6.616E-14	1.287	15.65
5.85E-05	1.048E-13	2.624	20.14
6.76E-05	1.619E-13	4.109	20.41
7.88E-05	2.565E-13	5.248	16.46
9.26E-05	4.161E-13	5.545	10.72
1.08E-04	6.589E-13	4.802	5.86
1.26E-04	1.043E-12	3.663	2.82
1.48E-04	1.693E-12	2.277	1.08
1.71E-04	2.617E-12	1.436	0.44
1.99E-04	4.144E-12	1.287	0.25
2.32E-04	6.563E-12	1.782	0.22
2.73E-04	1.065E-11	3.168	0.24
3.16E-04	1.646E-11	5	0.24
3.68E-04	2.606E-11	7.079	0.22
4.29E-04	4.127E-11	9.208	0.18
4.92E-04	6.227E-11	10.693	0.14
5.83E-04	1.035E-10	11.139	0.09
6.85E-04	1.679E-10	9.851	0.05
7.85E-04	2.534E-10	7.178	0.02
9.30E-04	4.211E-10	3.416	0.01
		Totals	**100.00**

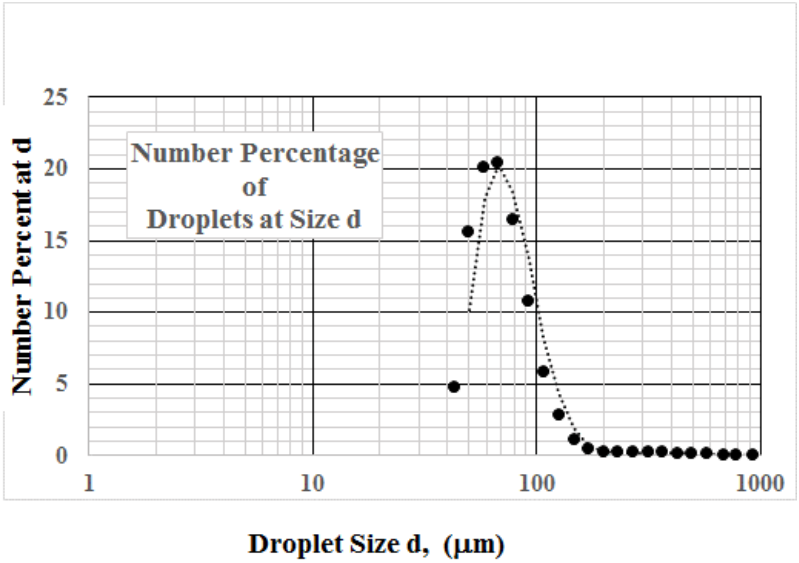

Fig. 6. Data of Fig. 5 cast in terms of number percent as described in text. Note the bimodal aspect of the data is no longer present and ~89% of the particles lie between 43 μm and 93 μm.

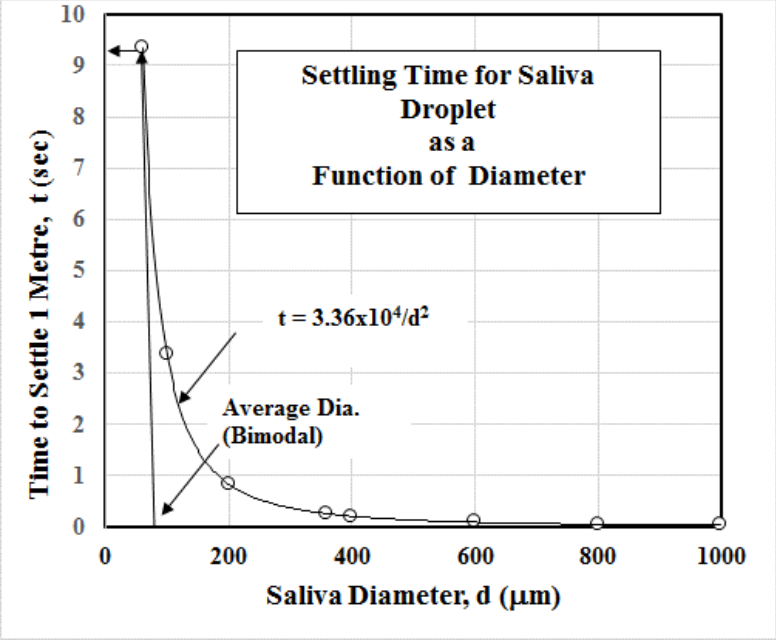

Fig. 7. Settling rate of saliva- encapsulated virions as a function of size. A representative value of about 60 µm was based on Fig. 6. Evaporation effects during settling are ignored.

b. Settling of Saliva-Encapsulated COVID-19 Virions – Evaporation Considered

Since evaporation of saliva during the settling of saliva-encased virions takes place, it is important to assess the extent to which it may be a factor in settling. The approach here is similar in philosophy to that of Wells [11], who considered whether a droplet evaporates before striking a surface at a given distance from the starting point. To assess the importance of evaporation, it is necessary to know how the size of saliva droplet changes with time using experimental data on the evaporation rate. Such data are given in Fig. 8 [12]. From Fig. 8 the saliva evaporation rate, C, is:

$C = -3.42 \times 10^{-9}\ m^2/s$ Eq. 2

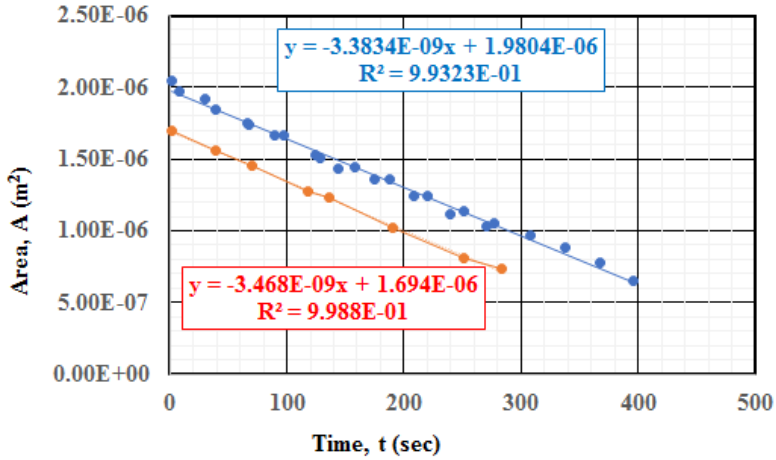

Fig. 8. Evaporation rate of saliva droplets at RT and 30% RH for 0.81 mm droplets (blue) and 0.78 mm droplets (red) [12]. Note the high degree of correlation of the best-fit lines with the data.

To calculate the continually slowing settling rate, due to the droplet becoming smaller from evaporation, we first examine the extent to which the droplet changes size over some reasonable time. To do this assume a spherical droplet of diameter D and constant surface evaporation rate (in m^2/s) of magnitude C.

The surface area of the droplet is:

$$A(t) = \pi D^2(t) \qquad \text{Eq. 3.}$$

From which

$$\frac{dA}{dt} = C = 2\pi D \frac{dD}{dt} \qquad \text{Eq. 4}$$

Assuming that *C* is in fact constant, as appears to be the case for the available data [12],[d] Eq. 4 can be integrated from the initial size *Do* at *t =0* to the size *D* at any time *t* with the result:

$$D = \sqrt{D_o^2 + \frac{Ct}{\pi}} \qquad \text{Eq. 5.}$$

For complete evaporation (i.e. *D ~ 0*) [e]

$$t = -\frac{\pi D_o^2}{C} \qquad \text{Eq. 6}$$

If there is some non-negligible concentration of virions in a drop, then the size at complete evaporation is fD_o where f <1 and is easily determined from the concentration. Thus in Eq. 6, D_o^2 would be replaced by $D_o^2(1 - f^2)$. [f] In the discussion below we assume that f ~ 0 for simplicity in illustrating the approach.

The Stokes Law evaporation-modified settling law is obtained by inserting Eq. 5 into Eq. 1[g]:

$$v = \frac{dx}{dt} = \frac{g\Delta\rho}{18\mu}\left(D_o^2 + \frac{Ct}{\pi}\right) \qquad \text{Eq. 7}$$

Where $\Delta\rho$ = difference in density between the virus and air.

Equation 7 is the time-mediated Stokes Law; it is seen that the velocity becomes essentially zero when the droplet is fully evaporated.

---

[d] Physically, the specific evaporation rate should actually increase with decreasing diameter based on increased surface energy.

[e] In this formulation the virus size is considered to be negligible with respect to the measured droplet sizes. Including the evaporation limit down to the virus size is easily done but has no effect on the results.

[f] This means an even shorter time to release "dry" virions since less evaporation would be required.

[g] It is assumed that the terminal velocity is established immediately at each instant of time. This assumption means that the settling times are, if anything, underestimated.

Equation 7 may be re-arranged and integrated from x = 0 (position at start of settling) at t=0 to any position x at time t with the result (See appendix A):

$$x = KD_0^2 t + \frac{KC}{2\pi} t^2 \qquad \text{Eq. 8}$$

Where $K = \frac{g\Delta\rho}{18\mu}$ Eq. 9

Again, the settling time to complete evaporation may be obtained by determining the value of t at which the maximum value of x occurs. This value turns out to be the same as was previously given in Eq. 6.

Equation 8, which includes evaporative effects, is plotted in Fig. 9 for 60 μm and 100 μm diameter sneeze droplets using data from the literature already presented (i.e. both C and that data used to calculate K from the physical constants which comprise it) and a value of 1.012 kg/m^3 as the density of saliva [13]. Qualitatively, the form of the curves is as expected, with the velocity, dx/dt, decreasing monotonically to zero with time.

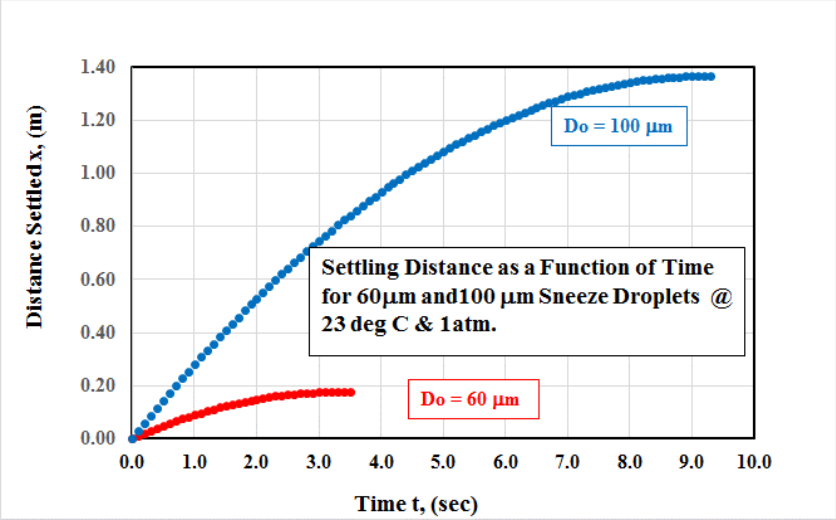

Fig. 9. Distance settled as a function of time for droplets sneezed in 30% RH air at 23ºC and 1 atm. Evaporative effects are considered and settling occurs only to the point of zero velocity (i.e. maximum distance and zero velocity, i.e. dx/dt =0.) At this point the virions are "dry". The curves are applicable only to the point at which evaporation is complete.

As expected, the larger droplets fall further and endure for longer times before complete evaporation. The time for the settling of the sneeze drop until complete evaporation is obtained by differentiation to find the time at maximum x. Differentiating and setting the derivative equal to zero yields, as required by the linkage between Eqns. 5,7 and 9, the same result as Eq. 6.

This result is substituted into Eq. 8 to obtain, after some manipulation:

$$x_{max} = K\frac{t_{max}}{2}D_o^2 \qquad \text{Eq. 10}$$

Values of the initial droplet size vs the settling time and distance are given in Table 3. Note that the plots shown in Fig. 9 agree with the corresponding data in Table 3.

Table 3. Settling Time for Complete Evaporation and Corresponding Settling Distance for Droplets of 60 μm and 100 μm diameter at 23 ^{o}C , 1 atm and 30% RH.

Droplet Diameter D (μm)	Maximum settling time, $t_{max} = -\pi Do^2/C$ (sec)	Maximum settling distance, $x = KDo^2t_{max}/2$ (m)
60	3.31E+00	1.77E-01
100	9.19E+00	1.37E+00

Table 2 shows that approximately 73% of all the droplets lie in the range from 60 μm to 100μm. Consequently, this range is considered to be representative of the behaviour of most of the saliva-covered droplets.

Effects of changes in relative humidity (RH) at 25^{o}C and 1 atm are easily calculated. For example, at about 38% RH, changes in the viscosity of air are minor [14] and changes in the density are negligible compared to the density of the COVID-19 virus. Using data from [12], at 38% RH, 23^{o}C and 1atm, C = -2.89 x 10^{-9} m^2/sec. Using this value, the settling times and distances respectively are 3.91sec and 0.21 m (60 μm droplets) . For 100 μm droplets the corresponding values are 10.9 sec and 1.62 m. Comparing with the values in Table 3 for 30% RH, changes in RH have a modest but significant effect in the range of interest. The directions of the changes are what one would intuitively expect; the less rapid evaporation at 38% RH should lead to longer evaporation times.

c. Effects of Temperature

Some idea of the effect of temperature may be obtained by examining the behaviour at 37 ^{o}C and 25% RH as shown in Fig. 10. Again, data from [12], for 25% RH, 37^{o}C and 1atm was used in constructing Fig. 10. In this case, C = -8.00 x 10^{-9} m^2/sec. Changes in air density and viscosity are very small compared to changes in the evaporation rate so only the different value of C was used. Using this value, the settling times and distances respectively are 1.4 sec and 0.076 m (60 μm droplets) . For 100 μm droplets the corresponding values are 3.9 sec and 0.58 m. Comparing with the values in Table 3 and Fig. 9, changes in temperature have a very large effect in reducing the settling times and distances, presumably releasing the virions very rapidly. To the extent that the virions remain viable at higher temperatures, increased temperatures could be more dangerous in spreading viable virions. More work is needed to determine the effect of temperature on COVID-19 viability. Again, the directions of the changes are what one would intuitively expect.

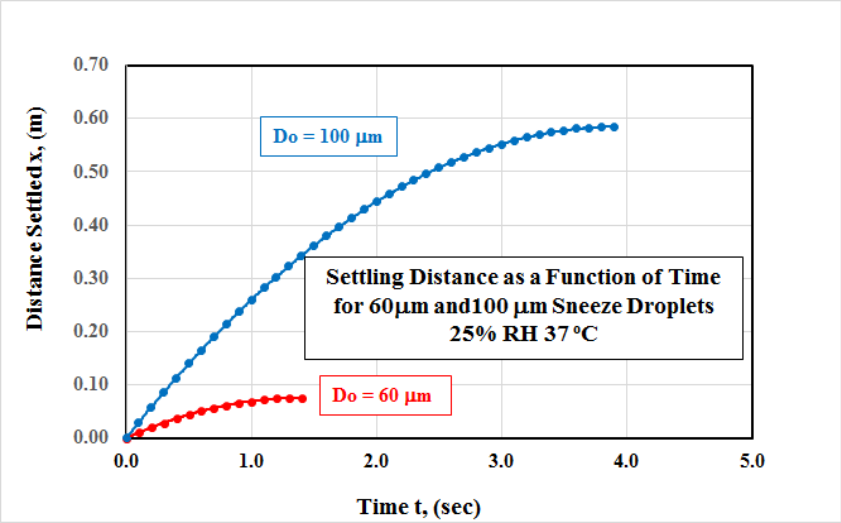

Fig. 10. Similar to Fig. 9 except for droplets sneezed in 25 % RH air at 37°C and 1 atm. Note the large effect of increased temperature on reducing both the time to complete evaporation and the distance settled. This means that increases in temperature will result in rapid release of virions from the droplets.

Based on the development of the time-mediated Stokes Law, experimental data for evaporation rates, the size distribution of droplets in a sneeze, and the previous discussion of settling of "dry" COVID-19 virions, it is likely that sneezing gives rise to a large number of virions in the local environment. It has been shown that most "wet" virions (i.e. in excess of 70%) will have evaporated before falling even 1 metre and thus are the source of "dry" virions in the local environment. Since the life of the virions is much longer than the release time (i.e. seconds vs hours) the released virions, unless somehow rendered neutral or blocked, can cause air-borne infection absent an effective vaccine. The picture that evolves is that droplets evaporate rapidly and are a source of dry virions. These results are in general agreement with those obtained by other investigators.[15] In addition, higher temperatures cause rapid evaporation and fast release of virions. Balanced against the rapid release would be the effect of temperature on COVID-19 life. Subsequent sections consider the efficacy of current approaches to masking as a way to block contact of COVID-19 with humans.

III. Masking and Movement of Covid-19

Masking has been widely suggested, or, in some cases, mandated, as a means of slowing or even stopping the physical spread of the COVID-19 virus. However, curiously enough, no quantitative target values for filtering out or blocking COVID-19 virions have been provided to date. Thus, it is not possible to say what constitutes success in terms of masking. A vast array of masks has been produced, many or even most, without any specific standards for designs, materials and fabrication methods. These designs and materials include bandanas, paper and cloth masks of unspecified nature, silk, nylon and, rarely, N-95 masks, said to be the "gold standard". Furthermore, government recommendations are to limit, to the extent possible, use of N-95 masks to health workers.

A. Examination of Masks Compared to Size of COVID-19

In the previous sections we have shown that sneezing and coughing are likely to be the source of viable, "dry" COVID-19 virions . The question naturally arises as to how populations might be protected against infection; use of masks is a natural response. In this section we examine the extent to which this approach could be effective by considering mask details, human breathing and filtration theory. A high magnification SEM photo of an N-95 mask is shown in Fig. 11 [16].

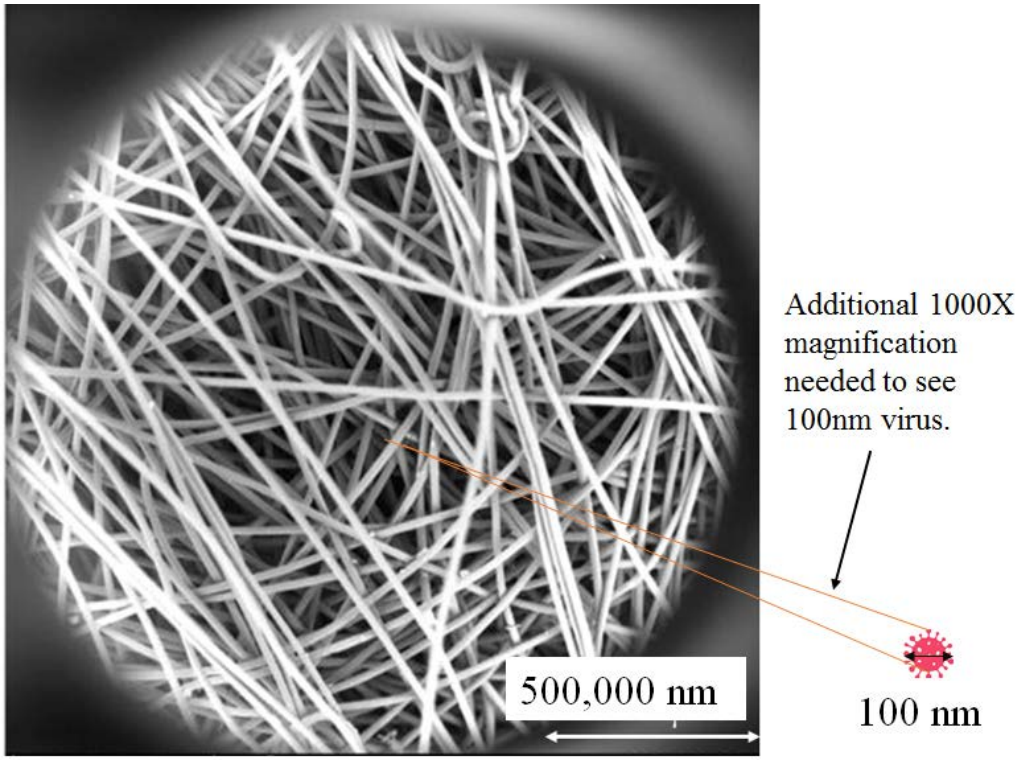

(a) (b)

Fig. 11. SEM micrograph of (a) N-95 mask and (b) schematic of typical COVID-19 virus. Note that the magnification in (b) is an additional 1000X higher than that in (a) in order to see the virus at the size in (b). Thus, it is seen directly that the COVID-19 virus is at least 2500X smaller than a large fraction of the holes in the mask. This micrograph raises the question of the ability of the N-95 mask to effectively stop virions from passing through it[h].

It is immediately obvious that the N-95 mask is porous and that the pores range from about 1,000 nm, to about 200,000 nm. While the multiple strands do not entirely block the virions, they could slow down their passage through the mask. The electro-static charge on the fibers aids the N-95 filtering process making particle penetration more difficult. All-in-all, the N-95 mask appears to

[h] As is well known, the N-95 mask has electro-statically treated fibers which helps in blocking virions. However, the charge "wears off" with use and time, rendering the mechanical filtering process relatively more important. The CDC has recommended that its use be limited to health workers, due to limited supplies.

be inadequate for efficient filtering of the COVID-19 virus as well as many, if not most, virus types shown in Table 4 at the 95% level. Some additional clinical studies are cited below. The usefulness of any mask, of course will depend on the critical viral load for infection which is not well defined at this time. A recent study[17] has concluded that:

> *"the median infection risk via aerosol transmission with one-hour exposure (10^{-6} to 10^{-4}) was significantly lower than the risk caused by close contact (10^{-1}) in a room of the area from 10 to 400 m^2 with one infected individual in it and with typical ventilation rate 1 ACH (Air Changes per Hour)".*

Table 4. Basic structural information for various virus types

virus	size (nm)	genome size (base pairs)	genome type, capsid structure	BNID
porcine circovirus (PCV)	17	1,760	circular ssDNA, icosahedral	106467, 106468
cowpea mosaic virus (CPMV)	28	9,400	2 ssRNA molecules, icosahedral	106454, 106455
cowpea chlorotic mottle virus (CCMV)	28	7,900	3 ssRNA molecules, icosahedral	106456, 106457
φX174 (*E. coli* bacteriophage)	32	5,400	ssDNA, icosahedral	103246, 106442
tobacco mosaic virus (TMV)	40×300	6,400	ssRNA, rod shaped	104376, 104375, 106453
polio virus	30	7,500	ssRNA, icosahedral	103114, 111324
φ29 (*Bacillus* phage)	45x54	19,000	dsDNA, icosahedral (T3)	109734
lambda phage	58	49,000	dsDNA, icosahedral (with tail)	103122, 105770
T7 bacteriophage	58	40,000	dsDNA, 55 genes, icosahedral (T7)	109732, 109733
adenovirus (linear DNA)	88-110	36,000	dsDNA, icosahedral	103114, 103115, 106441
influenza A	80-120	14,000	ssRNA, roughly spherical	104073, 105768
HIV-1	120-150	9,700	ssRNA, roughly spherical	101849, 105769
herpes simplex virus 1	125	153,000	dsDNA, icosahedral	103114, 106458
Epstein-Barr virus (EBV)	140	170,000	dsDNA, icosahedral	103246, 111424
mimivirus	500	1,200,000	dsDNA, icosahedral	105142, 105143
pandora virus	500x1000	2,800,000	dsDNA, icosahedral	109554, 109556

However, in Fig. 11, the COVID-19 virus is at least 20 times smaller than the smallest opening and more than 2500X smaller than a large number of the openings in this figure. The paper and cloth masks are also very open. Typical paper masks are shown in Fig. 12 [18] while a typical cloth mask is shown in Fig. 13 [19]. The open channels are on the order of the size of those in the N-95 mask. Nylon and silk masks are shown in Figs. 14 [20] and 15 [21] respectively. The kinds of masks shown in Figs. 12-15 are probably the most important to consider; they are by far the most frequently used, with, in addition, surgical masks (e.g. Fig. 12) being used both by medical personnel and the general public.

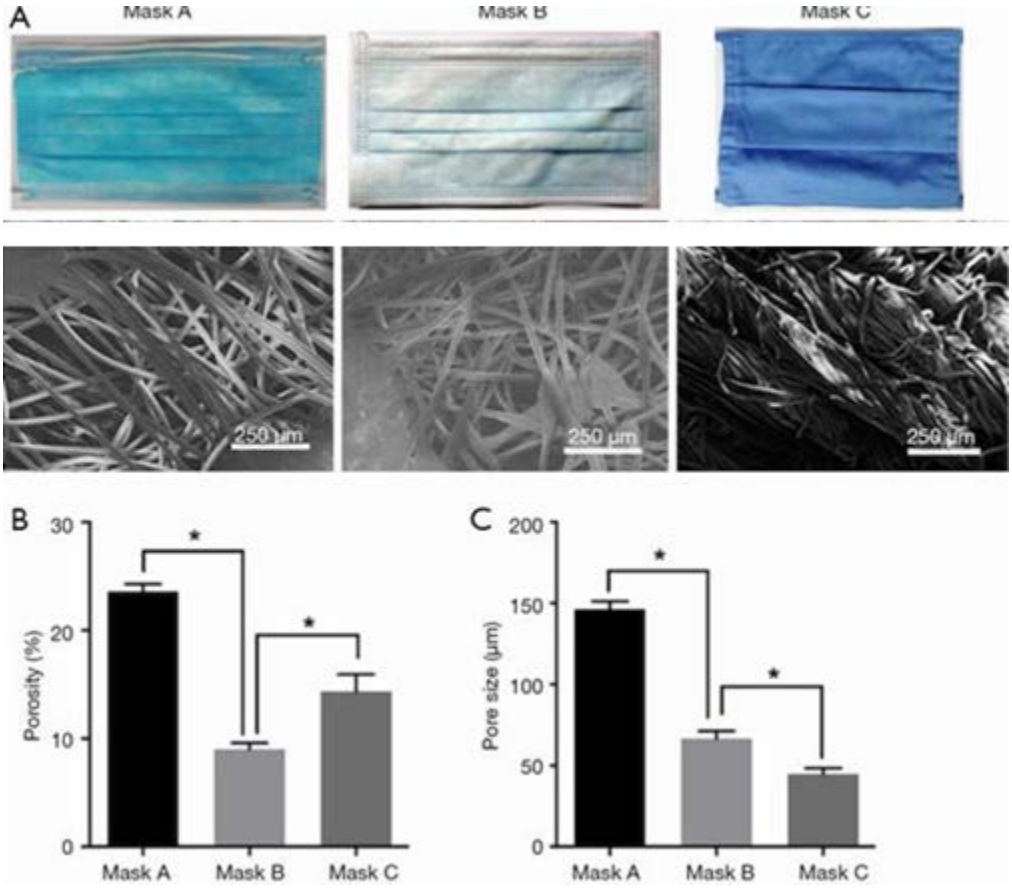

Fig. 12. A: three common disposable paper face masks with SEM micrographs of the individual masks. B: porosity of each mask. C: pore size of each face mask expressed in microns (1 micron = 1,000 nm) indicating that the COVID-19 virus at 0.06 to 0.14 µm would not be effectively filtered out by any of the three masks. Note for mask A the pore size is about 1500X larger than the average COVID-19 virus while for B and C the pores are 750 X and 400 X larger [18].

Fig. 13. Typical cotton weave mask [19]. At the cross overs, many of the larger void spaces in this micrograph are about 200,000 nm or about 2,000 X the size of the COVID-19 virus.

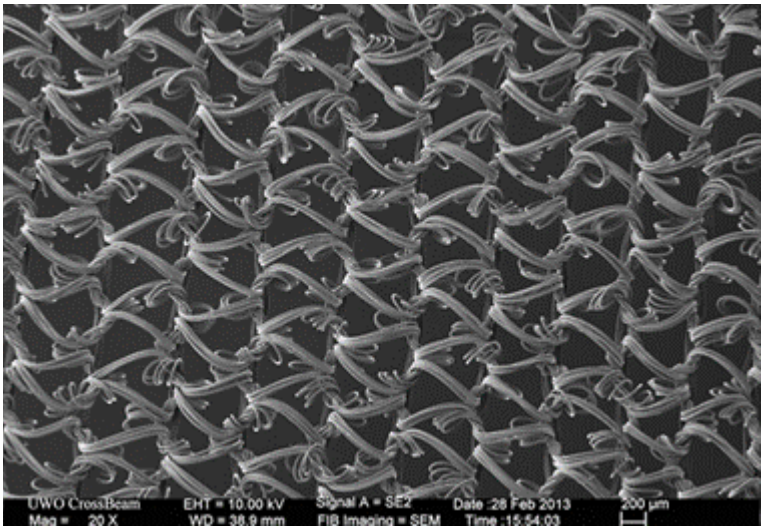

Fig. 14. Nylon showing voids at least 200,000 nm [20]. The open spaces are about 4,000X larger than the average COVID-19 virus.

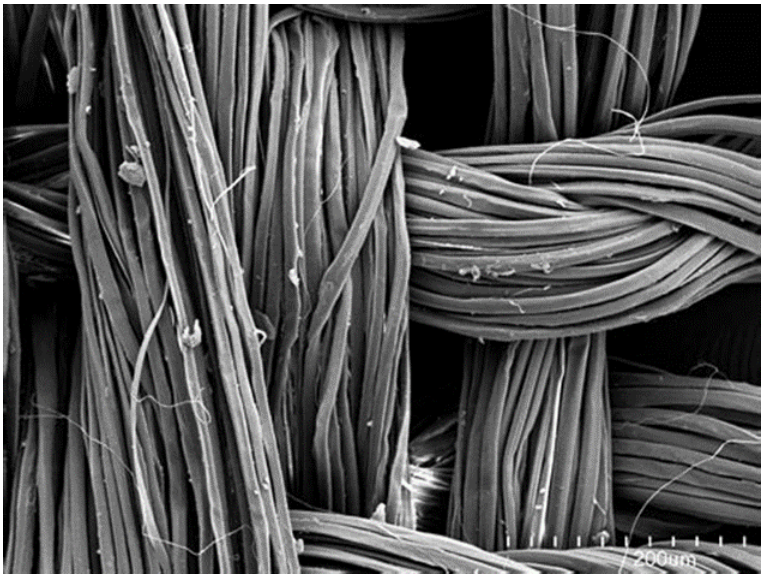

Fig. 15. Woven silk showing voids of about 50,000 nm – 100,000 nm or about 500X to 1,000X the average virus size [21].

Humans shed both "dry" and "wet" COVID-19 virions into the local environment by breathing, talking, coughing and sneezing. The preceding calculations have shown that even most of the "wet" virions are a source of "dry" virions through evaporation before hitting surfaces. It has also been shown that masking materials have numerous pores that are hundreds to thousands of times larger than the COVID-19 virions. These factors, ignoring blow-by effects, tend to call into serious question the strategy of using currently-available masks as a means of combatting infection by COVID-19, or indeed, by other virus types. A recent paper [22] also reports inconclusive clinical results on the effects of masking. It states, in part:

> "*Our results suggest that the recommendation to wear a surgical mask when outside the home among others did not reduce, at conventional levels of statistical significance, the incidence of SARS-CoV-2 infection in mask wearers. [This result was obtained] in a setting where social distancing and other public health measures were in effect. [However] mask recommendations were not among those measures, and community use of masks was uncommon. Yet, the findings were inconclusive and cannot definitively exclude a 46% reduction to a 23% increase in infection of mask wearers in such a setting.* [i] "

B. Masks and Important Factors in Filtration

The physics of fluid flow, called fluid mechanics, is a mature, well-established discipline in physics and in several engineering fields. It has helped to make possible our modern world. The part of fluid mechanics that concerns this paper is the theory of gas flow through a fibrous aerosol filter face mask, whether paper, polymer, cotton, silk, fiberglass, etc. For those readers interested, the theory of gas flow through porous media is well covered by Bear [23], Brown [24], Carman[25], Collins [26], S.J. Friedlander [27],S.K. Friedlander [28], Matteson [29], Muskat [30], Pich [31], and Scheidegger [32]. As with most products, scientific equipment, and measurements, a standard by which to judge an item or procedure is important. In science and engineering, the most common and universally accepted set of standards for a vast array of products, tests, and measurements are developed and published under the auspices of ASTM International. ASTM International, formerly the American

[i] Punctuation and a few words have been added [brackets] by the present authors for clarity.

Society for Testing and Materials, is the oldest established organization that develops and publishes technical standards in materials, systems, products and services. There are over 12,575 listed standards which are employed by governments, corporations, universities, and test laboratories worldwide. In the U.S., only the United States Pharmacopeia (USP), which has provided standards in the areas of medicine, biologics, food, supplements, and sterile compounding facilities (USP 795, 797, 800) for over 200 years, is older , while the British Pharmacopeia, which traces its origins back to King Henry VIII (1491-1547), is the oldest.

As was mentioned above, the N95 face mask is the undisputed "gold standard" for face masks and filtration of particulates. The National Institute for Occupational Safety and Health (NIOSH) approved N95 face mask must comply to with the following ASTM International standards:

- ASTM F2299/F2299M-03 (2017) Standard Test Method for Determining the Initial Efficiency of Materials Used in Medical Face Masks to Penetration by Particulates Using Latex Spheres

- ASTM F2101-19 Standard Test Method for Evaluating the Bacterial Filtration Efficiency (BFE) of Medical Face Mask Materials, Using a Biological Aerosol of Staphylococcus aureus

- ASTM F2100-19 Standard Specification for Performance of Materials Used in Medical Face Masks

- ASTM F1862/F1862M-17 Standard Test Method for Resistance of Medical Face Masks to Penetration by Synthetic Blood (Horizontal Projection of Fixed Volume at a Known Velocity)

The filtration standard for the N95 face mask is based on the bacteria Staphylococcus Aureus, shown in Fig. 16 [33].

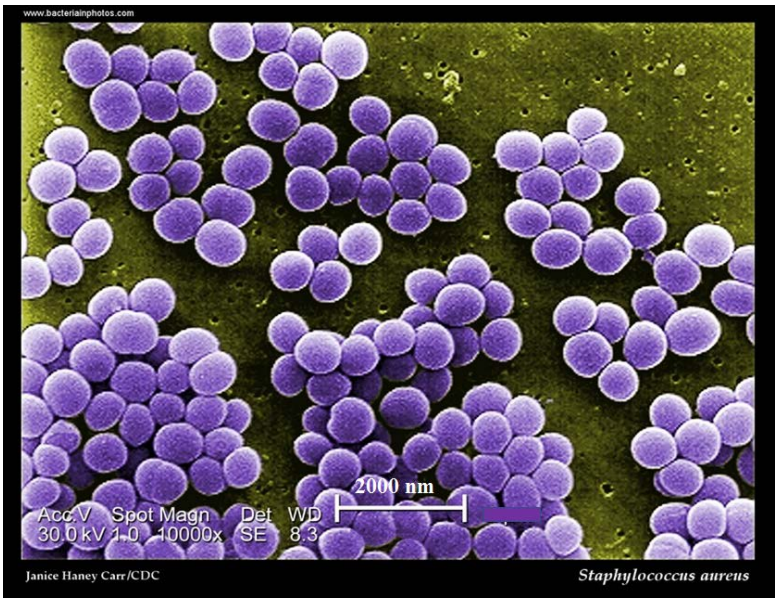

Fig. 16. SEM micrograph of Staphylococcus Aureus bacteria [33]. The diameter is about 700 nm, sufficiently large to be substantially filtered by an N-95 mask. The Staphylococcus Aureus bacteria is about 7X the size of the average COVID-19 virus.

The staphylococcus aureus bacteria are about 700 nm in diameter, far larger than the COVID-19 virus, which ranges in size from 60 nm to 140 nm as mentioned previously. Compare Fig. 16 to Fig. 11 and Fig. AC-1 in Appendix C.

There is no ASTM standard or any other international standard (e.g., British Standards BSI, International Electrotechnical Commission IEC, Deutsches Institut für Normung DIN, American National Standards AMNSI, American Petroleum Institute API, Association Française de Normalisation AFNOR, International Organization for Standards ISO, Japanese Standards Association JAS, Underwriters Laboratory UL) for a face mask that will filter out a virus. In fact, the N95 face mask will not even filter out proteobacteria (associated with most hospital acquired infections) in the size range of 300 nm to 600 nm, which like Staphylococcus Aureus, are huge compared to the SARS-CoV-2 virus (i.e. about 3-6X larger). Obviously, as seen in the photomicrographs in the preceding section, other masks may be even less effective than the N95 mask. More details on filtration are provided in Appendix B.

Some noteworthy testing on viral penetration of surgical and N-95 masks, fit tightly to manikins, was reported in 2006 by Anna Ba1azy et al. [34] using MS2 virions. It was shown that even absent leakage from an imperfect fit, the surgical masks were penetrated anywhere from 12-80% in the size range of about 80 nm, depending on the breathing rate and individual mask. The penetration for materials like nylon, silk and ordinary cloth, all of which have huge holes, will obviously be greater. The N-95 masks performed better (from 1-6% penetration) but again essentially just the masking material was tested. The blow-by (leakage), associated with mask fit and design, was not part of the study. These and other [35] authors recognized the importance of blow-by in a real-world setting where the sealing of the mask/face interface is imperfect at best. Coffey et al. [35] stated that without a good fit of a respirator to the individual face, the appropriate level of protection

cannot be obtained. The probable importance of leakage was further shown in a study done in Ontario, Canada comparing the effectiveness of surgical and N-95 masks in protecting health workers against influenza [36]. In this clinical study, 225 nurses received surgical masks and 221 got N-95 masks. Influenza infection occurred in 23.6% of the nurses with surgical masks and in 22.9% of those with N-95 masks.

C. Effect of Masks on Human Breathing

Human lung pressures and lung compliance are defined by the bulk air flowing into and out of the lungs along pressure gradients created in between the external environment and the alveoli [37],[38],[39]. The intra-pleural pressure at the commencement of inhalation is approximately -1.84 mm Hg (-2.5 cm H_2O) [40] . On average, a human has a respiration rate of 28.3 liters per minute (1 cubic ft./min) [37, 38, 39]. A high efficiency particulate air filter (HEPA), would typically be used for a Class 10,000 Clean Room (e.g., a clinical manufacturing facility for gene and cell therapy, a sterile compounding facility, a drug development lab, the nutraceutical industry, specialized electronic component production). In such a facility, no more than 10,000 particles per cubic metre (35.31 cubic ft.) of 300 nm or larger are allowed. For example, removing 99.97% to 99.995% of all particles larger than 500 nm using a Type H14 HEPA filter with a minimum of 10-25 air changes per hour ***would not filter out the COVID-19 virus at 60 to 140 nm in size***. According to the ISO 14644-1:2015, Clean Room Standards, there would still be a maximum concentration of 352,000 particles per cubic metre (35.31 cubic ft.) greater than or equal to 500 nm. For particles 1,000 nm and larger, there would be a maximum of 83,200 particles per cubic metre (35.31 cubic ft.) while for particles 5,000 nm and larger there would be a maximum of 2,930 particles per cubic metre (35.31 cubic ft.). To achieve these levels, the negative pressure and flow rates required are well beyond the capacity of the human lungs and the HEPA still would not filter out the COVID-19 virus. In fact, even a U 17 ultra-low particulate air filter (ULPA), the best filter available, would remove 99.999% + of contaminants 120 nm or larger in diameter but requires an extremely large negative pressure to pull air through this filter and requires large motors and fan blades running at very high rpm's.

D. Possible Improvements in Approaches to Masking

It has been shown that even with masking, there may be significant transmissions of COVID-19 virions, either dry or encapsulated by saliva.

Potential actions that might be usefully undertaken are:

- Define an objective goal for masks in terms of COVID-19 filtering. This would involve knowing critical concentrations of the COVID-19 virus that can cause infection in much of the population.

- Define materials, design and methods of fabrication to reach that goal. Without quantitative, measurable goals and standards for reaching them, considerable confusion and controversy will remain.

- Even with the current masks, there is obvious and considerable blow-by around the periphery of the mask. A simple step would be to provide a strip of tape around the periphery to attach to the facial skin to significantly reduce or even eliminate all blow by.

- Examine the possibility of making surface-active masks that will not only filter by physical blocking but that will also provide attraction between mask and virus, by chemical or additional novel electro-static means.
- Linked to the above and for electro-static "traps", develop sizes, spacings and charges that effectively target virions of the size range of concern.

IV. Suggestions for Further Research.

Some suggestions for further research into the way in which masking affects how COVID-19 virions can spread are:

- Examine the way in which the COVID-19 (and other) virions actually move through masks to determine the effectiveness of mask design and materials.
- Do full fluid flow computational studies of current masks to realistically determine how both "dry" and "wet" virions flow through masks currently in use (including design and materials) and around gaps in the masks on the periphery.
- Carry out simultaneous studies to examine how improved filtering affects human breathing, including oxygen and carbon dioxide levels in the body.
- The question arises as to the fraction of SARS-CoV-2 virions that are trapped by any kind of face mask. This can be determined in a straightforward way by:
    - Taking a known quantity of viable SARS-CoV-2 virions that have been tagged with a radioisotope.
    - Placing them in an air-tight glove box,
    - Employing a device to expel the SARS-CoV-2 viruses at 1 cubic foot per minute (normal breathing rate) onto the front of the fixed face mask.
    - Using three Geiger-Muller counters, each with an end window tube, count the irradiated viruses: (a) prior to just entering the face mask, (b) trapped by the mask, and (c) passing through the face mask.

  These experiments could bring certainty to the efficacy of any type of mask.

V. Summary and Conclusions

The purpose of this paper has been to examine: (a) the ways in which the COVID-19 virus can propagate and (b) the effectiveness of masking in preventing its spread. We have considered Stokes Law of settling for both "dry" and saliva-encapsulated ("wet") virions. In doing the latter, Stokes law has been modified to consider time dependence via evaporation of saliva-encapsulated COVID-19 virions. Finally, in light of our results, we have considered current efforts being used to meet the COVID-19 challenge via masking. In this regard, a summary comparing the sizes of pores in masks relative to the size of the COVID-19 virus has been provided with some comments. In particular, we have shown that:

- The average sized "dry" virus, 100/120 nm, takes more than 25 days to fall one metre. Since air currents, and other retarding factors, were ignored in this analysis, this result implies that "dry" virions are essentially always in the air.
- Given that the virus life in air has been reported to be from 0.64 to 2.64 hrs. with a mean of 1.09 hrs., a large fraction of the air borne virions in the environment are dead.

- The average size of saliva droplets from sneezes and coughs is about 60,000 nm. The saliva coating evaporates in a matter of seconds. Most droplets evaporate before falling 1 meter, thus providing a path for "dry" virions to enter the environment.
- Increases in the RH cause moderately slower evaporation of saliva-encapsulated virions, making striking low surfaces more probable.
- Increases in temperature cause very rapid increases in evaporation, leading to a release of "dry" virions from typical saliva droplets in very few seconds.
- Depending on the effect of temperature on virus life, higher temperatures may promote greater concentrations of "dry" COVID-19 virions into the local environment.
- There are no masks currently available that are certified by any international standards organization for filtering of COVID-19 virions nor are there any applicable standards for manufacturing and testing such masks.
- The requirements to filter COVID-19 virions exceed those currently in effect for filtering the air in medical level clean rooms. That is to say, present day clean-room technology would not effectively filter COVID-19 virions. Currently available masks would not be expected to give better results.

Acknowledgements: *The authors would like to thank: (1) Dr. H. Graeme French, MD, for useful discussions and for pointing out important references, (2) Prof. Albert W. Taylor of the faculties Medicine and Dentistry and the Faculty of Health Sciences at the University of Western Ontario for encouragement and for useful discussions and (3) Mr. Steven I. Gutstein, J.D., Esq . for reviewing the manuscript and for helpful suggestions.*

Appendix A

Some Comments on Computational Details of Equation 8 and Dynamic Formulation Including Evaporation

Equation 8, which includes evaporation, is obtained by straightforward integration of the velocity equation, Eq. 7:

$$v = \frac{dx}{dt} = \frac{g\Delta\rho}{18\mu}\left(D_o^2 + \frac{Ct}{\pi}\right) = KD_o^2 + \frac{CKt}{\pi} \qquad \text{Eq. A1}$$

The position of the COVID-19 virion goes from x =0 at t = 0 to x = x at some time t which is expressed mathematically through the integral equation:

$$\int_{x=0}^{x=x} dx = \int_{t=0}^{t=t}\left(KD_o^2 + \frac{CKt}{\pi}\right)dt \qquad \text{Eq. A2}$$

Which becomes Equation 8:

$$x = KD_0^2 t + \frac{KC}{2\pi}t^2 \qquad \text{Eq. A3}$$

Dynamic Formulation

The problem may be formulated more completely from a physics perspective by including the "ma" force. Using the convention that downward directed forces are positive, the forces acting on the virus are:

Shear drag force acting up (-)

$$F_s = -2\pi D\mu\frac{dx}{dt} \qquad \text{Eq.A4}$$

Pressure force acting up (-)

$$F_p = -\pi D\mu\frac{dx}{dt} \qquad \text{Eq. A5}$$

Gravitational force acting down on particle (+)

$$F_g = \frac{\pi D^3}{6}\rho_v g \qquad \text{Eq. A6}$$

Buoyancy force acting up (-)

$$F_g = \frac{\pi D^3}{6}\rho_a g \qquad \text{Eq. A7}$$

According to Newton's Second Law, the sum of these forces F_Σ , *plus the force associated with momentum advection*, may be equated to the mass x acceleration where by mass it is meant the total mass of the particle at any time t, *m(t)*:

$$F_\Sigma + F_p = m(t)\frac{d^2x}{dt^2} \qquad \text{Eq. A8}$$

Determination of the momentum advection force F_p could be a non-trivial exercise. We are currently considering this dynamic formulation to see if potential exists for new and important insights which will be reported, as appropriate, later.

Appendix B

Some Additional Comments on Filtration Theory

A filter is a porous media that separates dispersed particles from a dispersing fluid, which is either a gas or liquid [23,24,25,27,28,29,31]. The filtration process is characterized by several parameters, as follows:

1. Pressure drop (ΔP), where P_1 is the gas or liquid pressure before the filter and P_2 is the pressure behind the filter, as follows: $\Delta P = P_1 - P_2$. Pressure drop is a function of the fluid being filtered, the and properties of the porous media [23,24,25,27,28,29,31]. As the filtration process continues, the pressure drop becomes an additional function of the particulate matter deposited in and on the filter media [23,24,25,27,28,29,31].
2. Filter efficiency (E) for a mono-dispersed system is defined by:

$$E = \left(\frac{G_3}{G_1}\right) = \left(\frac{G_1 - G_2}{G_1}\right) = \left(\frac{G_3}{G_3 + G_2}\right) \quad \text{Eq. A9}$$

Where:

G1 = flux of particles flowing into the filter
G2 = flux of particles emitted by the filter and not trapped
G3 = is the portion of the particles trapped by the filter [23,24,25,27,28,29,31].

E is thus defined in terms of captured and incoming matter, the second term of entering and exiting particles, and the third term defined as retained particles and exiting ones. A related quantity is the penetration (P_n) of the filter media:

$$P_n = 1 - E. \quad \text{Eq. A10}$$

The reduction in particle concentration after passing through the filter (P^*) can be defined as [23,24,25,27,28,29,31]:

$$P^* = P_n^{-1} = (1 - E)^{-1} \quad \text{Eq. A11}$$

3. The filter quality (Q^*) is used to compare the quality of different filters, where the higher the Q^* value, the more efficient the porous media is at filtering [8]: $Q^* = -\ln P / \Delta P$.

The science and engineering of fluid mechanics has validated several mechanisms relevant to the deposition of particles from a flowing fluid, whether it be a gas or liquid. The most important are [23,24,25,27,28,29,31]:

1. Diffusion deposition
2. Direct particle interception
3. Inertial deposition
4. Gravitational deposition
5. Electro-Static deposition

6. London-van der Waal deposition
7. Capture coefficients

The structure of fibrous filters can be described and quantified by the following ten parameters [23,24,25,27,28,29,31]:

1. Fiber diameter
2. Fiber diameter distribution
3. Fiber concentration
4. Fiber porosity
5. Shape of the fibers
6. Pore size
7. Pore distribution
8. Spatial arrangement of the fibers
9. Specific surface
10. Filter porosity

The preceding discussion is provided to summarize some of the basic principles of filtration science and engineering that must be considered to understand and produce filters. The production of an efficient filter for a given application is complex, lengthy and costly. Before engaging in such a process, integration of physics, chemistry and engineering principles, such as attempted in this paper, must indicate a high probability for a successful outcome.

Appendix C

COVID-19 in Human Lung

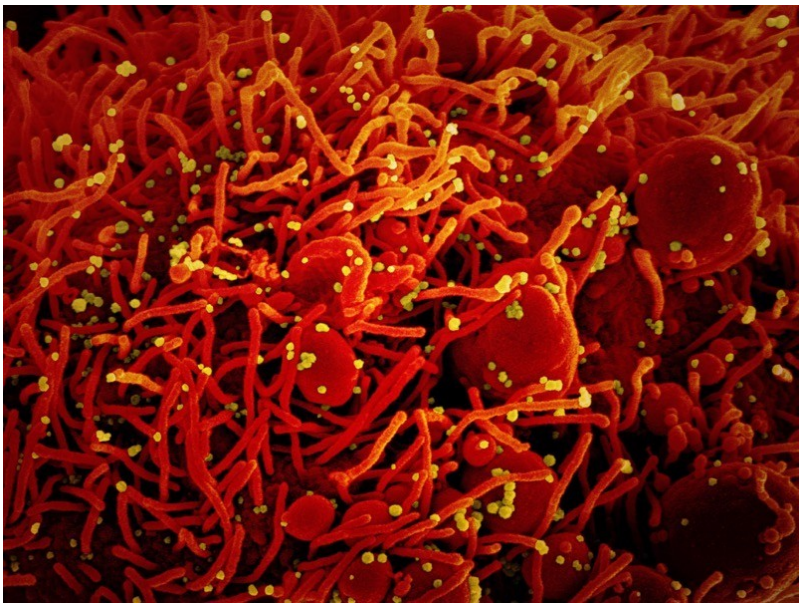

Fig. AC-1. False-colored SEM image. The large red quasi-spheroidal objects are eosinophilic cells (10,000 to 12,000 nm), a type of leukocyte (i.e., white blood cell) and the small yellow objects are the COVID-19 viruses (60-140 nm). Source: The Integrated Research Facility (IRF), Fort Detrick, Maryland a division of the National Institute of Allergy and Infectious Diseases (NIAID). False coloring, used to produce striking visual effects, can make the virions appear to be either larger or smaller than in reality.

Appendix D

Suggested Further Reading

C. M. Case, (1994), Physical Principles of Flow in Unsaturated Porous Media, Oxford University Press, New York.

B. R. Munson, D. F. Young, and T. H. Okiishi, (2005), Fundamentals of Fluid Mechanics, Fifth Edition, John Wiley & Sons, Hoboken, New Jersey.

R. W. Fox, P. J. Pritchard, and A. T. McDonald, (2009), Introduction to Fluid Mechanics, Seventh Edition, John Wiley & Sons, Hoboken, New Jersey.

L. D. Landau and E. M. Lifshitz, (1987), Fluid Mechanics, Volume 6 Landau and Lifshitz Course of Theoretical Physics, Pergamon Press, Oxford, U.K.

C. A. Tidona, G. Darai , and C. Buchen-Osmond (Editors), (2001),The Springer Index of Viruses, Springer-Verlag, Heidelberg, Germany.

K. J. Ryan and C. George Ray (Editors), (2014), Sherris Medical Microbiology, Sixth Edition, McGraw Hill Medical, New York.

D. R. Boone, G. M. Garrity (Editors) along with 8 other Editors, and 105 authors, (2001), Bergey's Manual of Systematic Bacteriology, Second Edition, Volume I: The Archaea and the Deeply Branching and Phototrophic Bacteria, Springer-Verlag, Heidelberg, Germany.

D. J. Brenner, Noel R. Krieg, J. T. Staley, and G. M. Garrity (Editors), along with 8 other Editors and 339 authors, (2005), Bergey's Manual of Systematic Bacteriology, Second Edition, Volume II, Part A: The Proteobacteria, Introductory Essays, Springer-Verlag, New York.

D. J. Brenner, Noel R. Krieg, J. T. Staley, and G. M. Garrity (Editors), along with 8 other Editors and 339 authors, (2005), Bergey's Manual of Systematic Bacteriology, Second Edition, Volume II, Part B: The Proteobacteria, The Gamma-Proteobacteria, Springer-Verlag, New York.

D. J. Brenner, Noel R. Krieg, J. T. Staley, and G. M. Garrity (Editors), along with 5 other Editors and 222 authors, (2005), Bergey's Manual of Systematic Bacteriology, Second Edition, Volume II, Part C: The Proteobacteria, The Alpha-, Beta-, Delta- and Epsilon-Proteobacteria, Springer-Verlag, New York.

D. H. Crawford, (2018), Viruses: A Very Short Introduction, Second Edition, Oxford University Press, Oxford, U.K.

T. Shors, (2016), Understanding Viruses, Third Edition, Jones, Bartlett Learning, Burlington, M.A.

P. Lostroh, (2019), Molecular and Cellular Biology of Viruses, CRC Press, an Imprint of Taylor & Francis Group, Boca Raton, Florida.

M. J. Roossinck, (2017), Virus, Ivy Press, an Imprint of Quarto Publishing, Princeton University, Princeton, New Jersey.

C. Zimmer, (2015), A Planet of Viruses, Second Edition, The University of Chicago Press, Chicago.

H. Quinlan, (2020), Plagues, Pandemics and Viruses: From the Plague of Athens to COVID-19, Visible Ink Press, Canton, Michigan.

M. B. A. Oldstone, (2020), Viruses, Plagues & History: Past, Present, and Future, Oxford University Press, Oxford, U.K.

D. Axe, William M. Briggs ,and J. W. Richards (2020), The Price of Panic: How the Tyranny of Experts Turned a Pandemic into a Catastrophe, Regnery Publishing, an Imprint of Salem Media Group, Washington, D.C.

T. Engelbrecht and K. Claus, (2020), Virus Mania: Corona/COVID-19, Measles, Swine Flu, Cervical Cancer, Avian Flu, SARS, BSE, Hepatitis C, AIDS, Polio: How the Medical Industry Continually Invents Epidemics, Making Billion-Dollar Profits at Our Expense, emu-Verlag, Lahnstein, Germany.

Dennis G. Zill and W. S. Wright, (2014), Advanced Engineering Mathematics, Fifth Edition, Jones & Bartlett Learning, Burlington, M.A.

References

[1] Na Zhu + 17 additional authors: A Novel Coronavirus from Patients with Pneumonia in China, NEJM, Vol. 382, January 24, 2020, pp. 727-733 DOI: 10.1056/NEJMoa2001017
[2] K. Nassau, (1983), The Physics and Chemistry of Color, John Wiley & Sons, New York.
[3] R. Feynman, R. Leighton and M. Sands, (1964 & 2010), The Feynman Lectures on Physics, Volume II, Basics Books an Imprint of Perseus Book Group, New York.
[4] G. G. Stokes: (1851). On the effect of internal friction of fluids on the motion of pendulums. Transactions of the Cambridge Philosophical Society, vol. 9, part ii: pp. 8–106. Bibcode:1851TCaPS...9....8S. The formula for terminal velocity (V) appears on p. [52], equation (127).
[5] See, for example, Wikipedia , https://en.wikipedia.org/wiki/Stokes'_law
[6] Yinon M Bar-On, Avi Flamholz, Rob Phillips and Ron Milo: SARS-CoV-2 (COVID-19) by the numbers, eLife 2020;9:e57309. DOI: https://doi.org/10.7554/eLife.57309.
[7] https://www.engineersedge.com/physics/viscosity_of_air_dynamic_and_kinematic_14483.htm
[8] D. G. Sharp, A. R. Taylor, I. W. McLean, Jr., Dorothy Beard, and J.W. Beard: Densities and sizes of the influenza viruses A (PR* strain) and B (Lee strain) and the swine influenza virus, J. Bio. Chem, vol. 159, 1945, pp. 29-44.
[9]N. van Doremalen, T. Bushmaker, D.H. Morris +10 additional authors: Aerosol and Surface Stability of SARS-CoV-2 as Compared with SARS-CoV-1, N. Engl. J. Med. 382;16 nejm.org April 16, 2020 (See in particular the Appendix to the letter.)bioDOI: 10.1056/NEJMc2004973
[10] Z. Y. Han, W. G. Weng and Q. Y. Huang: Characterizations of particle size distribution of the droplets exhaled by sneeze, R. Soc. Interface vol. 10, 2013: 20130560. http://dx.doi.org/10.1098/rsif.2013.0560
[11] W. F. Wells: On air-borne infection—Study II droplets and droplet nuclei. Am. J. Hyg., vol. 20, 1934, pp. 611–618 .
[12] T. Zhang: Study on surface tension and evaporation rate of human saliva, saline, and water droplets (2011). MS Thesis, University of West Virginia, Thesis Graduate Theses, Dissertations, and Problem Reports. 2271. https://researchrepository.wvu.edu/etd/2271
[13] Elżbieta Kubala, Paulina Strzelecka, Marta Grzegocka, Danuta Lietz-Kijak, Helena Gronwald, Piotr Skomro, and Edward Kijak: A Review of Selected Studies That Determine the Physical and Chemical Properties of Saliva in the Field of Dental Treatment, BioMed. Res. Intl., vol. 2018 ,2018, pp. 1-13. .doi.org/10.1155/2018/6572381.
[14] P.T. Tsilingiris: Thermophysical and transport properties of humid air at temperature range between 0 and 100 ^{o}C, Energy Conversion and Management, vol. 49, 2008, pp.1098–1110.
[15] Roland R. Netz and William A. Eaton: Physics of virus transmission by speaking droplets, https://www.pnas.org/cgi/doi/10.1073/pnas.2011889117
[16] SEM Micrograph from Masks meet Science: University of New Mexico's School of Mechanical Engineering (Manufacturing Training and Technology Center) based on Professor Pavel Lushnikov's research on the physics of masks. Featured in the Monday, April 6, 2020 Albuquerque Journal's article, Masks meet Science by Kevin Robinson-Avila. SEM taken on April 2, 2020 at 15:31.
[17] Xiaole Zhang and Jing Wang: Dose-response Relation Deduced for Coronaviruses from COVID-19, SARS and MERS Meta-analysis Results and its Application for Infection Risk Assessment of Aerosol Transmission https://pubmed.ncbi.nlm.nih.gov/33119733/
[18] Zhiqing Liu, Degang Yu, Yuwei Ge, Liao Wang, Jingwei Zhang, Huiwu Li, Fengxiang Liu, Zanjing Zhai: Understanding the factors involved in determining the bioburdens of surgical masks, *Ann Transl Med* 2019;7(23):754 | http://dx.doi.org/10.21037/atm.2019.11.91
[19] University of Western Ontario Western Nano Fabrication Laboratory.
[20] University of Western Ontario Western Nano Fabrication Laboratory. Taken by Todd Simpson of the UWO Nano-fabrication Facility, 2013.
[21] Vartest laboratories. http://vartest.com/category/silk/
[22] Henning Bundgaard +21 additional authors: Effectiveness of Adding a Mask Recommendation to Other PublicHealth Measures to Prevent SARS-CoV-2 Infection in Danish Mask Wearers: A Randomized Controlled Trial, Ann Intern. Med. doi:10.7326/M20-6817 Annals.org 18 November 2020.
[23] J. Bear, (1973), Dynamics of Fluids in Porous Media, American Elsevier Publishing Company, Inc., New York. ISBN: 0-486-65675-6. https://doi.org/10.2136/sssaj1973.03615995003700040004x.

[24] R. C. Brown, (1993), Air Filtration: An Integrated Approach to the Theory and Applications of Fibrous Filters, 1st Edition, Pergamon Press, Oxford, U.K., an Imprint of Elsevier. ISBN: 13: 978-0080412740.
[25] P. C. Carman, (1956), The Flow of Gasses Through Porous Media, Academic Press, New York. ASIN: B0000CJFSN, UNSPSC-Code: 55101500. https://doi.org/10.1177/004051755902900112.
[26] R. E. Collins, (1961), The Flow of Fluids Through Porous Materials, Reinhold Publishing, New York. https://doi.org/10.1002/aic.690080102.
[27] S. J. Friedlander and D. Serre, (2007), Handbook of Mathematical Fluid Dynamics, Volumes 1-4, North Holland Publishing Company, an Imprint of Elsevier, Amsterdam, The Netherlands.
[28] S. K. Friedlander: Theory of Aerosol Filtration, Ind. Eng. Chem. 1958, 50, 8, 1161-1164. https://doi.org/10.1021/1e50584a036.
[29] M. J. Matteson and C. Orr, Editors, (1987), Filtration: principles and Practices, Second Edition, Marcel Dekker, Inc. New York.
[30] M. Muskat, (1937), The Flow of Homogeneous Fluids Through Porous Media, McGraw-Hill, New York.
[31] J. Pich, (1966), in Aerosol Science (C. N. Davies, ed.), Academic Press, New York.
[32] A. E. Scheidegger, (1957), The Flow of Fluids Through Porous Media, University of Toronto, Toronto, Canada.
[33] Janice Haney Carr/CDC: SEM micrography of Staphylococcus Aureus bacteria. Public domain photo. http://bacteriainphotos.com/Staphylococcus aureus electron microscopy.html
[34] Anna Balazy, Mika Toivola, Atin Adhikari, Satheesh K. Sivasubramani, Tiina Reponen, and Sergey A. Grinshpun: Do N95 respirators provide 95% protection level against airborne viruses, and how adequate are surgical masks?, AJIC, Vol. 34, 2006, pp. 51-57.
[35]Christopher C Coffey, Robert B Lawrence, Donald L Campbell, Ziqing Zhuang, Catherine A Calvert, Paul A Jensen: Fitting characteristics of eighteen N95 filtering-facepiece respirators. J Occup Environ Hyg vol. 1, 2004, pp. 262-271.
[36] Mark Loeb, Nancy Dafoe, James Mahony, Michael John, Alicia Sarabia, Verne Glavin, Richard Webby, Marek Smieja, David J D Earn, Sylvia Chong, Ashley Webb, and Stephen D Walter: Surgical mask vs N95 respirator for preventing influenza among health care workers: a randomized trial, JAMA vol. 302, 2009, pp.1865-1871. doi: 10.1001/jama.2009.1466.
[37] J. B. West and A. M. Luks, (2016), West's respiratory Physiology: The Essentials, Tenth Edition, Lippincott, Williams and Wilkins an Imprint of Wolters Kluwer, Philadelphia, Pennsylvania.
[38] S. E. Weinberger, B. A. Cockrill and J. Mandel, (2018), Principles of Pulmonary Medicine, Seventh Edition, Elsevier, Philadelphia, Pennsylvania
[39] P. D. Scanlon and R. E. Hyatt, (2020), Hyatt's Interpretation of Pulmonary Function Tests: A Practice Guide, Fifth Edition, Lippincott, Williams and Wilkins an Imprint of Wolters Kluwer, Philadelphia, Pennsylvania.
[40] R. J. Mason, et al. (authors), V. C. Brodddus (Editor), (2015), Murray & Nadel's Textbook of Respiratory Medicine, Volumes I & II, 6th Edition, Elsevier, Amsterdam, The Netherlands.